ELSEVIER

Journal of Alloys and Compounds 348 (2003) 23–29

Journal of ALLOYS AND COMPOUNDS

www.elsevier.com/locate/jallcom

Heat conductivity of valence doped $La_{0.7}Ca_{0.3}Mn_{1-x}Fe_xO_{3-\delta}$

A.M. Ahmed[a,1], M. Boshta[c], R. Braunstein[c], V. Morchshakov[a], K. Bärner[a,*], C.P. Yang[a,2], J.R. Sun[b], G.H. Rao[b]

[a] *IV Physikalisches Institut, Georg-August-Universität, Bunsenstrasse 11–15, D-37073 Göttingen, Germany*
[b] *Institute of Physics, Chinese Academy of Sciences, Beijing 100080, PR China*
[c] *UCLA Physics Department, 405 Hilgard Ave., Los Angeles, CA 90024, USA*

Received 6 May 2002; received in revised form 27 May 2002; accepted 27 May 2002

Abstract

The temperature dependences of the resistivity ρ and the heat conductivity κ of $La_{0.7}Ca_{0.3}Mn_{1-x}Fe_xO_{3-\delta}$ ($0<x<0.12$) fixed valence doped crystals were studied between 50 and 340 K using the time resolved thermoelectric effects (TTE-method). The heat conductivity κ is dominated by the lattice contribution and changes from a crystalline to a randomized scenario with increasing Fe-content. We also observe a splitting of the Curie and metal–insulator transition temperature $T_c > T_{mi}$ which we assign mainly to a small oxygen deficit in the TTE-measured sample surface layer. Steps in κ at T_{mi}, $\Delta\kappa_{mi}$, are assigned to polaronic effects. $\Delta\kappa_{mi}$ changes sign with increasing x, suggesting that Fe–Fe pairs in octahedral settings take over from the single Fe-sites (dilute limit) already at $x=0.04$. For $x>0.06$, structures in $\kappa(T)$ suggest that larger Fe-based clusters are introduced.

Keywords: Rare earth compounds; Transition metal compounds; Electrical transport; Heat conduction; Phase transition

1. Introduction

The unusual physical properties of the mixed valence compounds with perovskite structure $R_{1-x}A_xMnO_3$ have aroused a lot of interest since the discovery of giant magnetoresistance effects (GMR) in this class of compounds [1–3]. The manganites are also very attractive from a fundamental point of view, as the interactions and the transport in this type of compound are not fully understood as yet. In former contributions, it has been found that the increasing substitution of Fe for Mn results in an increase in the resistivity and a decrease in the metal–insulator transition temperature T_{mi}, both of which have been related to Zener bond blocking [4,5]. The concept of Zener bond blocking has been introduced in Ref. [6] after it has been realized that for the Mn^{3+}–Mn^{4+} Zener pair to build a resonant state in perovskite crystals, one needs an additional qualification, i.e. according to Ref. [6], both ions have to be completely surrounded by octahedra which contain a Mn^{3+} ion. That yields in particular a maximum Curie temperature T_c at $x=0.33$, which is close to experiment. Also, a decrease in T_c follows when fixed valence ions like Fe^{3+} are substituted for Mn, as more and more Zener bonds lose their qualification. A slightly different qualification has been proposed in Ref. [4], pointing out that one has to take into account that with increasing x, usually $R_{0.5}A_{0.5}MnO_3$ limits the existence region of double exchange ferromagnets and not $AMnO_3$. This leads to the following prediction for the doping dependence of T_c, at least at small x [4]:

$$T_c/T_{co} = (1 - 1.429x)(1 - 6x) \quad (1)$$

While this concept obviously explains the decrease in T_c with x, and is consistent with the increase in the resistivity, its applicability concerning the heat conductivity $\kappa(x)$ is uncertain as yet. If, for example, the Wiedemann–Franz law were valid in the metallic region, κ should also decrease with x.

Therefore, in this contribution, we have measured the heat conductivity of $La_{0.7}Ca_{0.3}Mn_{1-x}Fe_xO_3$ ceramic sam-

*Corresponding author. Fax: +49-551-394560.
E-mail address: baerner@ph4.physik.uni-goettingen.de (K. Bärner).
[1] Present address: Physics Department, South Valley University, Sohag, Egypt.
[2] Present address: Department of Materials Science and Engineering, Tsinghua University, Beijing, PR China.

0925-8388/02/$ – see front matter
PII: S0925-8388(02)00826-5

ples. We find that the absolute values of κ are more or less independent of x, suggesting from the start that the lattice contribution probably dominates the heat conductivity. However, at the metal–insulator transition temperature, T_{mi}, we find a step $\Delta\kappa_{mi}$ which undergoes a sign reversal with increasing x and other structure in $\kappa(T)$, both of which have to be addressed.

2. Experimental

2.1. Sample preparation

Polycrystalline samples of nominal composition $La_{0.7}Ca_{0.3}Mn_{1-x}Fe_xO_3$ were synthesized by standard solid state reaction methods. Stoichiometric proportions of La_2O_3, $CaCO_3$, MnO_2 and Fe_2O_3 were mixed and then reacted in air at 1173 K for 24 h. The product thus obtained was reground, pelletized and sintered at 1473 K for 96 h with intermediate grinding and pelleting, and then cooled slowly to room temperature. Before mixing the raw materials, commercial La_2O_3 was dehydrated at 1073 K for 24 h, then weighed and exposed to air for 4 days. X-Ray powder diffraction patterns (XRD) indicated that single phase samples were obtained for $x \leq 0.12$ [4]. The single phase samples crystallize in an orthorhombically distorted perovskite structure with space group *Pbnm* and the lattice parameters increase only slightly with increasing Fe-substitution. For a preliminary sample characterisation, the temperature dependences of the resistivity were measured in a cryostat using the d.c. four-contact method, and general agreement was found with literature data [4,5].

2.2. Time resolved thermoelectric effects (TTE-method)

For this report we have applied the TTE-method to measure the heat diffusivity D of the Fe-doped La–Ca manganites. The heat conductivity κ is then calculated using $D = \kappa/\rho_o c_v$ (ρ_o: density) and taking $c_p \approx c_v$. The specific heat capacity data $c_p(T)$ of these particular samples are found in Ref. [4]. Aside from the decay function of the TTE-transient from which D is derived, the TTE-(initial) amplitude simultaneously measures the thermoelectric power S; these TEP-data have been discussed in a different context [7]. Usually, T_{mi} can be identified both in D and S, as the TEP is supposed to drop and the heat conduction to increase on going into the metallic state. Curiously, with the manganites, T_c shows up in S only, suggesting a strong contribution of the spin system to the TEP, but a small one to the heat conductivity; however, in the heat diffusivity D one can easily detect T_c via the downward peak which stems from the magnetic peak in $c_p(T)$. One can in particular leave this downward peak as a T_c-marker in $\kappa(T)$ by separating c_p into a magnetic and a lattice part; this is done by fitting a Debye function to the experimental specific heat capacity (Fig. 1). Using the fit

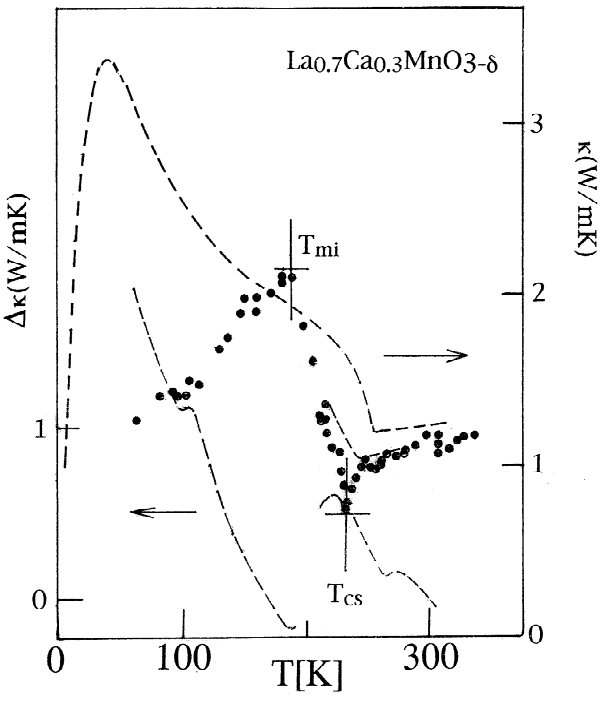

Fig. 1. Heat conductivity $\kappa(T)$ of $La_{0.7}Ca_{0.3}MnO_{3-\delta}$. Upper dashed curve (1): bulk measurement with $\delta = 0$ according to Ref. [8]; points (2): surface measurement with $\delta \approx 0.01$. T_{mi}, T_{cs}: metal–insulator and Curie temperatures in a surface layer (of ≈ 4 μm); lower dashed line: heat conductivity difference of curves (1) and (2); short dashed line: heat diffusivity $D \rightarrow \kappa$ conversion with full $c_p(T)$; for more details see text.

for the $D \rightarrow \kappa$ conversion, the T_c-marker will remain; of course, the marker is gone once one uses the full c_p-data. The data acquisition and reduction were carried out using Labview 5.2.

As an example, we present $\kappa(T)$ of the mother compound $La_{0.7}Ca_{0.3}MnO_3$ (Fig. 1). While at high temperatures our $\kappa(T)$ is close to that of Refs. [8,9], our Curie temperature is somewhat lower, as indicated by the dip in $\kappa(T)$ (points: lattice only $c_p(T)$—dashed line around T_c: full $c_p(T)$). That small shift in T_c is also found in the thermopower [7,10]. On the other hand, the increase in κ near T_c appears to be sharpened and shifted downward compared to the literature [8]. The upper dashed line in Fig. 1 is supposed to be a bulk measurement on LCMO with $T_{mi} = T_c$ [8]. All this suggests a split of T_c and T_{mi} in our measurement. The discrepancy with the literature has been resolved as follows: the TTE-method (also called light flash method) measures in a surface layer of about 4 μm of our sample, which has been found to contain surface stresses and/or an oxygen deficiency [10]. That causes the split of the Curie and metal insulator transition temperature, $T_{cs} > T_{mi}$. Moreover, at intermediate temperatures we observe a positive slope $d\kappa/dT > 0$ in contrast to $d\kappa/dT < 0$ for the bulk measurement [8], which suggests a randomisation in the TTE-measured surface layer; that is why we support an oxygen deficiency as the main cause of both the T_c-shift and the T_c/T_{mi} splitting. Having gone that

far, we can estimate a deficit of $\delta_1 \approx 0.01$ from a comparison of our T_c-shift to those of nominally oxygen deficient manganites [11].

3. Results

3.1. Conductivity and heat conductivity

Fig. 2 shows the resistivity versus temperature curves $\rho(T) = 1/\sigma$ and Fig. 3 the heat conductivity κ of the series $La_{0.7}Ca_{0.3}Mn_{1-x}Fe_xO_3$ with $x = 0$, 0.02, 0.04, 0.06, 0.08, 0.1, 0.12.

The resistivity $\rho(x, T)$ is in general consistent with the literature [4,5]: $\rho(T)$ runs over a maximum which is supposed to signal the metal–insulator transition at T_{mi}. Moreover, the Fe-substitution results in an increase in the resistivity and a decrease in T_{mi}. Note, however, that with ceramic samples $\rho(T)$ usually shows a double peak, which is resolved here only for $x = 0$. The first sharp peak signals T_c—the arrows in Fig. 2 are taken from direct magnetization measurements [4]. With non-doped compounds, it is generally believed that T_c and T_{mi} coincide. This, however, is difficult to ascertain with ceramic samples, as a second and broader peak usually occurs (see $\rho(T)$ of $x = 0$). This secondary maximum is thought to be connected with a particular (spin-dependent) scattering on grain boundaries [12,13], but it may also hide a split of T_{mi} and T_c. On the other hand, the $\rho(T)$-measurements are done in the bulk, where we could well have an oxygen-stoichiometry and with it $T_{mi} = T_c$. With the doped compounds, we have to assume a superposition of two peaks, too. That might cloud the exact position of T_{mi} and certainly makes a discrimination between metallic and semiconducting state through the slope of $\rho(T)$ difficult. Thus, an independent indicator of T_{mi} and the metallic state, like we expect to have in $\kappa(T)$, would be welcome.

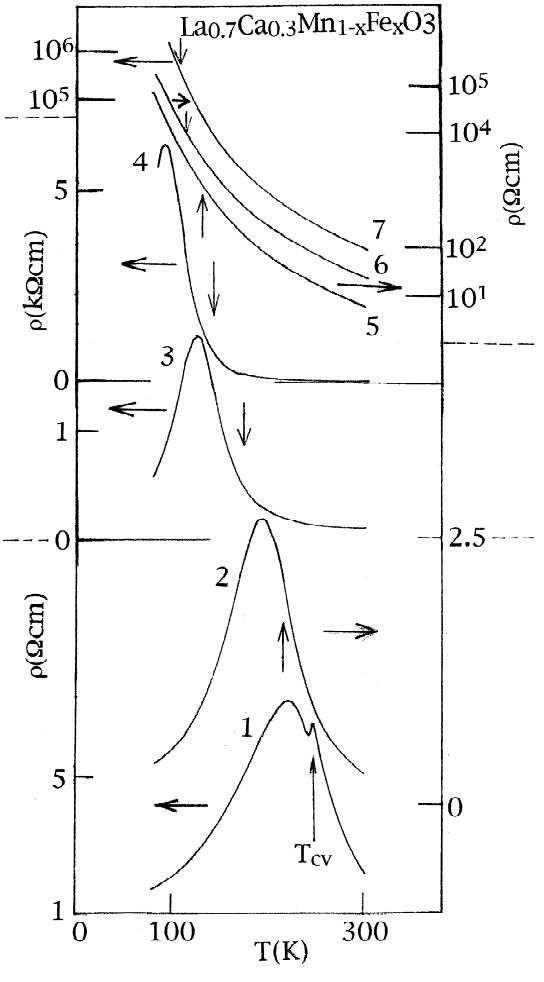

Fig. 2. Bulk resistivity versus temperature curves $\rho(T)$ of $La_{0.7}Ca_{0.3}Mn_{1-x}Fe_xO_3$ compounds with $x = 0$, 0.02, 0.04, 0.06, 0.08, 0.10, 0.12; T_{cv} (and arrows) Curie temperature in the volume.

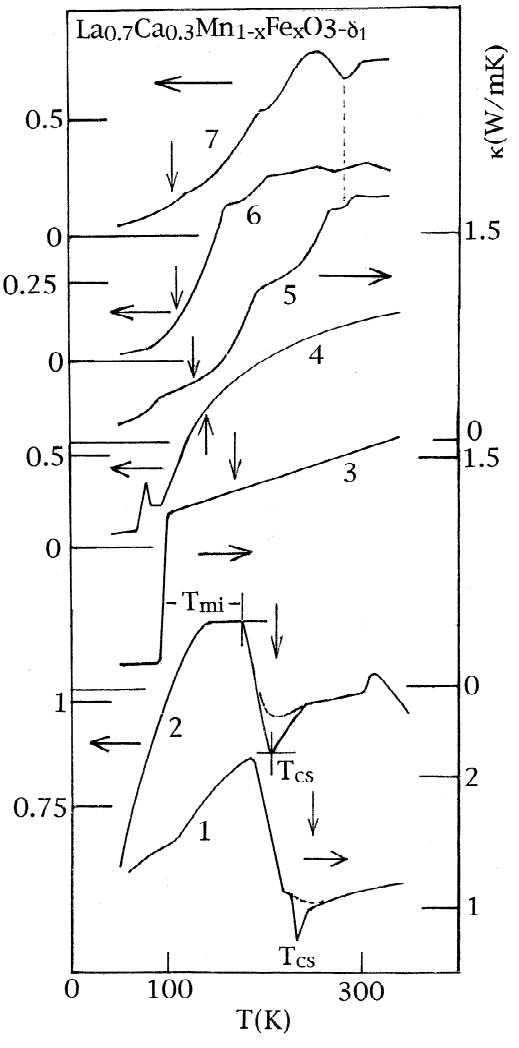

Fig. 3. Surface layer heat conductivity $\kappa(T)$ for $x = 0$, 0.02, 0.04, 0.06, 0.08, 0.10, 0.12 ($\delta_1 \approx 0.01$); arrows: T_{cv} from magnetisation measurements [4].

Fig. 3 shows $\kappa(T)$ for the same series of compounds. The mother compound (curve 1; $x = 0$) has already been discussed in connection with the description of the TTE-

measurement and a shift and split of T_{mi} and T_c have been concluded, probably arising from an oxygen non-stoichiometry near the sample surface. We detect a similar behaviour of $\kappa(T)$ in (a surface layer of) the compound with $x=0.02$, but now all transition temperatures are lower. This is most likely due to the influence of Fe. In both cases, we have left the T_c-marker on, so that the splitting of T_{mi} and T_c is visible. For $x\geq 0.04$, we lose the marker, as due to the increasing chemical randomisation, the magnetic peak in $c_p(T)$ is increasingly reduced [4]. However, the arrows still show the Curie temperatures as obtained from the (bulk) magnetisation curves. Close to the sample surface they are supposed to be somewhat smaller, $T_{cs}<T_c$, because of the oxygen deficit, which is supposed to also reside in the surface layers of the Fe-doped samples. Even then a slight increase in the splitting due to the Fe-doping cannot be ruled out (see curves 3,4). For the higher Fe-contents ($x\geq 0.08$; curves 5–7), we cannot detect T_{mi} anymore. Either T_{mi} is below the temperature range measured ($T\geq 50$ K), or the metallic state has disappeared at all. Note, that the step of κ at T_{mi}, $\Delta\kappa_{mi}$, gets reduced with increasing Fe-content (curves 1, 2), and switches sign on going from $x=0.02$ to $x=0.04$ (curves 2,3); for $x>0.04$ it gets smaller again (curves 3,4). This sign change of the step is supported by the behaviour of the TTE-amplitude, which is basically a measure for the thermoelectric power. While for $x=0$, the TEP is negative in the temperature range measured, at $x=0.02$ it is virtually zero at all T; at $x=0.04$, a larger $S(T)$ reappears, but with the sign changed to positive for temperatures above T_{mi} [7].

Before one applies the Wiedemann–Franz law, one might argue that one cannot compare the bulk $\rho(T)$ data with the $\kappa(T)$ data measured closer to the surface. However, as the absolute values of κ are still close with both types of measurement (Fig. 1), this is still possible as long as we stay with order of magnitude arguments. For the higher Fe-contents (curves 4–7), $\kappa(T)$ develops structure which might have to do with an increasing inhomogeneity.

4. Discussion

4.1. Conductivity

Only qualified Zener bonds contribute a mobile (polarised Zener-) carrier. If those bonds overlap in a percolative way, one will find metallic conduction. At the same time, only qualified Zener bonds provide a double exchange ferromagnetic coupling, and that is why we find the well-known correlation of ferromagnetism and metallic conduction which is the trademark of the manganites. Based on this strong electron–magnon coupling (double exchange) one can infer a correlation of conduction and magnetism also for the paramagnetic state: because the spin-dependent transfer now meets thermally fluctuating local spin moments S, the Zener–Anderson pair electronic states $E_{ij}=-JS\pm b\langle\cos\theta_{ij}\rangle$ (J: intraatomic exchange energy, b: spin-independent transfer integral, θ_{ij}: localized spin pair angle) will also fluctuate, which would yield a (magnetic) hopping type of conduction, i.e. a gapless insulating state [2]. Adding electron–phonon coupling, not only can one introduce a real gap, but the octahedra around the Mn^{3+}–Mn^{4+} pair get locally distorted (polaron picture [14]). If the metal–insulator transition and T_c coincide, $T_{mi}=T_c$, in the insulating state we expect to have fluctuations of these distortions, too, which adds a structural component to the hopping. Far into the metallic regime, $T<T_c$, the distortions should finally go into a coherent mode (just like ferromagnetism and metallicity), while close to T_{mi} we should still find fluctuations of this structural type, in an amount as described by an (secondary) order parameter. Disregarding the grain boundary scattering, the $\rho(T)$-curves of Fig. 2 are compatible with those ideas.

If T_{mi} and T_c separate, we introduce a transitional regime where there is a phase mixture or where one of the phases remains metastable. Again, because of the interference of grain boundary scattering, we cannot deduce either case from our $\rho(T)$ measurements.

When there is bond-blocking through single site Fe, not only does the carrier concentration go down, but the scattering is supposed to increase both via the introduction of Fe-spin related scattering potentials and their distortive byproducts. The gap values change by a factor of two only (Table 1), and thus the increase in the resistivity with x has to be mainly connected with the prefactor ρ_o [15].

Electronic gap values can be approximately obtained from an Arrhenius plot of the right-hand slope of the resistivity curve $\rho(T)$ (insulating state I). The Arrhenius fit usually gives too low values for the (mobility type of) gap. Indeed, the activated regime is best described by a Mott-like equation: $\ln(\rho/\rho_o)=(T_o/T)^{1/n}$, which only for $n=1$ and $kT_o=\Delta\varepsilon$ goes over to an Arrhenius law. Nevertheless, the effective (polaronic) gap value $\Delta\varepsilon$ which can be extracted using an Arrhenius fit should correlate with the splitting of T_c and T_{mi}, if such is found. In Ref. [15] in particular, it has been shown that with electron–phonon coupling added to mixed double exchange–superexchange magnetic coupling, it holds:

$$T_{mi}/T_o - T_1/T_o = -\Delta\varepsilon/2b \quad (2)$$

Table 1
Resistivity gap values and selected resistivity and thermal conductivity values

Fe-content	ρ_{max} (Ω cm)	$\Delta\varepsilon(\rho)$ (meV)	κ (300 K) (W/mK)
$x=0$	7.05	65	1.15
$x=0.02$	2.7	98	1.02
$x=0.04$	1.85 (kΩ cm)	70	1.56
$x=0.06$	6.2	60	1.23
$x=0.08$	–	140	1.78
$x=0.10$	–	96	0.63
$x=0.12$	–	120	0.73

where $T_o = 4NzJ_{ab}S^2/\alpha$, α is the entropy drop-off coefficient at T_1, N the atom number, z the coordination number, J_{ab} the negative superexchange integral, S the spin moment and b the spin-independent transfer integral. T_1 is the afm–fm order–order temperature, which replaces T_c when mixed afm and fm (double exchange) couplings are present. According to Fig. 3 and Table 1 indeed both the splitting and the effective gap values go up slightly with the Fe-doping.

4.2. Heat conductivity

Unlike the electrical conductivity, $\sigma(T)$, the heat conductivity $\kappa(T)$ is not significantly different in ceramic or single crystals [13,16,17], suggesting that the influence of grain boundaries is smaller here. This in turn supports again a predominance of the heat transport via the phonon system.

Specifically, the heat conductivity κ is usually written as a sum of lattice, spin lattice and electronic contributions:

$$\kappa = \kappa_l + \kappa_e + \kappa_m \quad (3)$$

Even with the best conducting (semi-) metallic state, $x=0$ at 50 K, the effective Lorentz number, $L = \kappa/\sigma T$, is only 1.15×10^{-7} $W\Omega/K^2$, i.e. L stays way above the electron heat conduction only value $L_o = 2.45\times10^{-8}$ $W\Omega/K^2$; also, there is no correlation of $\kappa(x, T)$ and $\sigma(x, T)$ as would be if the Wiedemann–Franz law were valid. That means: $\kappa_e \ll \kappa$. But what about κ_m? Now, since T_c and T_{mi} are split, one can look for steps at either transition separately. We find that T_c is barely detectable in $\kappa(T)$ of the mother compound, and that there is even less structure at T_c with the Fe-doped compounds, which means that $\kappa_m \ll \kappa$ in all cases, too. Accordingly, we have to discuss $\kappa(T)$ in terms of the phonon spectra. The temperature dependence of the lattice contribution κ_l usually goes over a broad maximum, since $\kappa_l \to 0$ for $T \to 0$ and $\kappa_l \sim T^{-n}$ at high temperatures where phonon–phonon (umklapp-) processes dominate the lattice heat conduction. Such a behaviour is actually found for the bulk mother compound $La_{0.7}Ca_{0.3}MnO_3$ [8,9] (Fig. 1), except for the cut at $T_{mi} = T_c$. The $\kappa(T)$-curve actually looks very much like a convolution of the conventional lattice heat conduction function and an order parameter function, which gives us a first hint that the polarons which arise out of the double exchange situation under an electron–phonon coupling, play a role here. As argued above, the polarons should undergo a transition at $T_c = T_{mi}$, too. Then, with T_{mi} and T_c split like in our surface layers, the polaron part should shift to T_{mi}, as is indeed observed (Fig. 1), and the spin polaron part to T_c. Moreover, from the sharpness of the step at T_{mi} we conclude that the transition now has turned from second to first order. But what about the sign change of $\Delta\kappa_{mi}$ with increasing x?

4.3. Fe–Fe pairing

Unexpectedly, it is the Zener bond blocking model which offers a way out. For Ge-doped compounds of the same class, $La_{0.7}Ca_{0.3}Mn_{1-x}GeO_3$, it has been found that T_c decreases up to $x=0.02$ and then increases again up to $x=0.04$ [18]. The initial drop has been explained in terms of Zener bond blocking via single site Ge, while an octahedral pair Ge–Ge adjacent to the Mn^{3+}–Mn^{4+} Zener pair constitutes a new resonant state, thus renewing the bond qualification. What if, equivalently, Fe–Fe pairs come into play at $x=0.04$ due to some attractive Fe–Fe pair interaction (see Fe_2O_3), but without forming a new resonant state? Instead, they continue to block the Zener bonds like single site Fe. In that case, one would not expect to find steps in a magnetisation or conductivity versus x dependence (at a given T) nor with $T_c(x)$ or $T_{mi}(x)$. However, one would certainly expect to see a change in the polaron spectrum caused by the pairing tendency. In particular, single sites and double sites might react differently to the metal–insulator transition in a local distortive way (static or dynamic polarons) as is independently supported by the sign change of the (spin polaronic) TEP between $x=0.02$ and $x=0.04$ [7].

4.4. Cluster modes

For $x \geq 0.04$, the slope of $\kappa(T)$ remains positive for all temperatures, suggesting an increasingly chemically (or elastically) randomized system. As we already used Fe–Fe pairs to explain the unusual features of $\kappa(T)$ found at lower Fe-contents, we expect the Fe-clustering tendency to increase at higher x. Indeed, for $x \geq 0.04$, we increasingly find structure in $\kappa(T)$ which we accordingly assign to Fe-related clusters. The replacement of Fe for Mn seems to have a strong influence on the phonon spectra of these compounds. We may even be able to identify some of the major cluster modes using the temperature dependence of the phonon mean free path $l \sim 1/T$ [19] at moderate temperatures:

$$\kappa = (1/3)Cvl \approx \text{const.}/T \quad (4)$$

where C, heat capacity; v, phonon velocity. The product κT being approximately constant, suggests to plot the difference between the heat conductivities of an ideal homogeneously Fe-distributed sample, κ_h, and a clustered sample, κ_c, times the temperature, i.e. $T(\kappa_c - \kappa_h) = T\Delta\kappa$, versus temperature T. Since an oxygen deficit also changes the phonon spectrum significantly, we can apply the same plot to the mother compound. Here we can take the literature bulk values for κ_h, while for the Fe-doped compounds we simply take a constant in T, relying on the fact that the increased chemical randomisation will tend to turn the slope $d\kappa_h/dT$ of a homogeneously Fe-distributed sample from negative to near zero. This has been done in Fig. 4.

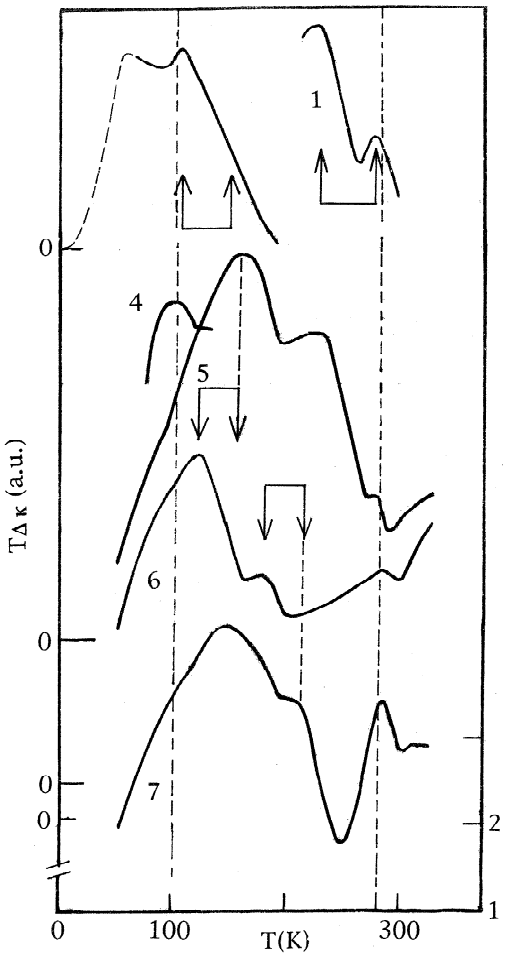

Fig. 4. $T(\kappa_c - \kappa_h)$ versus temperature T; the plot is supposed to show the major oxygen deficiency and Fe-clustering related oscillatory modes.

For the mother compound surface layer, we find indeed smaller but sharper structures, which we tentatively assign to oxygen defect oscillatory modes. These structures remain when we dope with Fe, suggesting that the surface layer retains its deficit with all samples. With increasing x, more and broader peaks appear, but once a new peak comes in at a certain Fe-content x, it appears to remain at all higher x (see arrows), consistent with the assumption of an increasing Fe-clustering, starting from Fe–Fe octahedral pairs.

Raman and IR-absorption experiments [20,21] are planned in order to more directly correlate the development of the heat conductivity with that of the cluster oscillatory modes.

4.5. Electronic–magnetic phase diagram

The characteristic temperatures which could be extracted from the magnetic and transport properties are collected in a phase diagram (Fig. 5). Note, that in the surface layer of all compounds, including the mother compound, T_c and T_{mi} are split, with $T_{mi} < T_c$, and are positioned a little

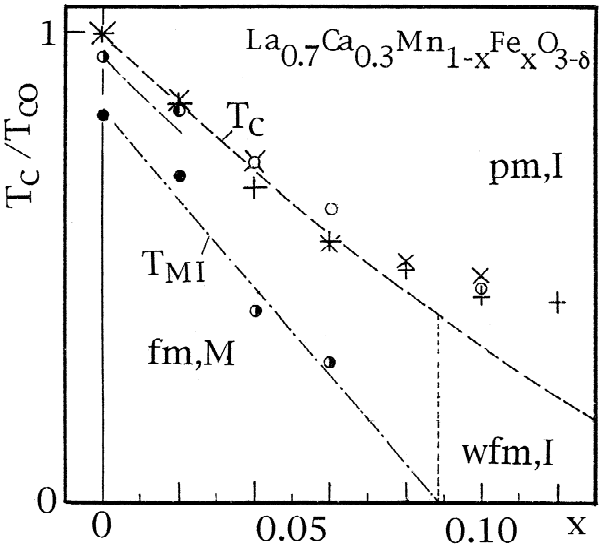

Fig. 5. Electronic–magnetic phase diagram of $La_{0.7}Ca_{0.3}Mn_{1-x}Fe_xO_{3-\delta}$. T_c, Curie temperature; upper dashed–dotted line: surface (T_{cs}); $\delta \approx 0.01$; upper dashed line: bulk (T_{cv}) calculated; points $\delta \approx 0$; T_{mi}, metal–insulator transition temperature (surface); wfm: weak ferromagnet; I: insulator; M: metal; pm: paramagnet; +: magnetisation [4]; ×: magnetoresistance [7]; ○,●: TTE-transients; amplitude or relaxation time (full points).

lower than the bulk values. Consistently, the metallic phase dies out before the cooperative magnetism does. In particular, $T_c(x)$ as given by Eq. (1) (slightly curved dashed–dotted line) fits the experimental points rather well except for larger x, where clustering is supposed to occur. In contrast, $T_{mi}(x)$, while starting with almost the same slope, as expected, remains more or less linear.

This in turn suggests that an insulating magnetically ordered phase (weak ferromagnet) is introduced (for $x > 0.095$) which eventually goes over to a magnetically inhomogeneous, spin-glass like situation for large Fe-doping, consistent with the increasing introduction of competing superexchange magnetic couplings, Fe^{3+}–Fe^{3+}, Fe^{3+}–Mn^{3+}, Fe^{3+}–Mn^{4+}.

Acknowledgements

The authors thank the Deutsche Forschungsgemeinschaft (DFG), the Alexander von Humboldt Foundation and the NATO linkage-grant PST.CLG.975703 for their support.

References

[1] J.M.D. Coey, M. Viret, S.v. Molnar, Adv. Phys. 48 (1999) 1.
[2] K. Bärner, Materials with a large magnetoresistance—some unifying aspects, TRN/MSE/8, Transworld Research Network, 2002, Trivandrum, India, in press.
[3] M. Imada, A. Fujimori, Y. Tokura, Rev. Mod. Phys. 70 (1998) 1039.
[4] G.H. Rao, J.R. Sun, A. Kattwinkel, L. Haupt, K. Bärner, E. Schmitt, E. Gmelin, Physica B 269 (1999) 379.

[5] S.K. Hasanain, M. Nadeem, W.H. Shah, M.J. Akhtar, M.M. Hasan, J. Phys. C 12 (2000) 9007.
[6] J.B. Goodenough, Phys. Rev. 100 (1955) 564.
[7] A.M. Ahmed, A. Kattwinkel, K. Bärner, C.P. Yang, J.R. Sun, G.H. Rao, Physica B 324 (2002) 102.
[8] J.L. Cohn, J.J. Neumeier, C.P. Popoviciu, K.J. McClellan, Th. Leventouri, Phys. Rev. B56 (1997) R8495.
[9] D.W. Visser, A.P. Ramirez, M.A. Subramanian, Phys. Rev. Lett. 78 (1997) 3947.
[10] K. Bärner, P. Mandal, A. Kattwinkel, A.M. Ahmed, R.V. Helmolt, J.R. Sun, G.H. Rao, Physics Metals Metallogr. 91 (2001) S164, ISSN 0031-918X.
[11] H.L. Ju, J. Gopalakrishnan, J.L. Peng, Q. Li, G.C. Xiong, T. Venkatesan, R.L. Greene, Phys. Rev. B 51 (1995) 6143.
[12] H.L. Ju, C. Kwon, Q. Li, R.L. Greene, T. Venkatesan, Appl. Phys. Lett. 65 (1994) 2108.
[13] S. Uhlenbruck, B. Büchner, R. Gross, A. Freimuth, A. Maria de Leon Guevara, A. Revcolevschi, Phys. Rev. B 57 (1998) R5571.
[14] A.J. Millis, P.B. Littlewood, B.I. Shraiman, Phys. Rev. Lett. 74 (1995) 5144.
[15] K. Bärner, P. Mandal, R.v. Helmolt, Phys. Status Solidi (b) 223 (2001) 811.
[16] H. Fujishiro, M. Ikebe, Physica B 263–264 (1999) 691.
[17] I. El-Kassab, A.M. Ahmed, P. Mandal, K. Bärner, A. Kattwinkel, U. Sondermann, Physica B 305 (2001) 233.
[18] A.M. Ahmed, A. Kattwinkel, J.R. Sun, G.H. Rao, H. Schicketanz, P. Terzieff, I.V. Medvedeva, K. Bärner, J. Magn. Magn. Mater. 242–245 (2002) 719.
[19] Ch. Kittel, Introduction to Solid State Physics, 6th Edition, Wiley, New York, 1986, ISBN 0-471-87474-4.
[20] E.R. Giessinger, R. Braunstein, E. Ladzinsky, L. Haupt, J.W. Schünemann, K. Bärner, U. Sondermann, A.F. Andresen, Solid State Commun. 78 (1991) 503.
[21] L. Haupt, R.v. Helmolt, U. Sondermann, K. Bärner, Y. Tang, E.R. Giessinger, E. Ladizinsky, R. Braunstein, Phys. Lett. A 165 (1992) 473.